THE ASTROPHYSICAL JOURNAL, 489:314–318, 1997 November 1

HOPKINS ULTRAVIOLET TELESCOPE OBSERVATIONS OF H_2 EMISSION FROM HH 2

JOHN C. RAYMOND
Harvard-Smithsonian Center for Astrophysics, 60 Garden Street, Cambridge, MA 02138; jraymond@cfa.harvard.edu
WILLIAM P. BLAIR
Department of Physics and Astronomy, Johns Hopkins University, Charles and 34th Streets, Baltimore, MD 21218; wpb@pha.jhu.edu.edu
AND
KNOX S. LONG
Space Telescope Science Institute, Baltimore, MD 21218; long@stsci.edu
Received 1997 April 7; accepted 1997 June 11

ABSTRACT

The Hopkins Ultraviolet Telescope spectrum of HH 2 shows Lyman band emission below 1200 Å, and it reveals H_2 bands in the quasi-continuum at longer wavelengths. The H_2 emission could arise either from Lyα fluorescence (as in other HH objects) or from collisional excitation by hot electrons. The fluorescence hypothesis encounters some difficulty in explaining the lack of individual strong features, while the collisional hypothesis must explain the mixing of hot electrons into the molecular gas before photoionization or collisions with H atoms dissociate the molecules. The spectrum also provides a stringent upper limit to the O VI flux. The upper limit appears to conflict badly with the predictions of bow-shock models that match the observed line widths of HH 2A′ and HH 2H.

Subject headings: molecular processes — shock waves — stars: pre–main-sequence — ultraviolet: stars

1. INTRODUCTION

As two of the brightest Herbig-Haro objects in the sky, HH 1 and HH 2 provided some of the earliest spectral evidence that HH objects are shock waves (Schwartz 1977) and the first tests of bow-shock models for their emission-line intensities and profiles (Hartmann & Raymond 1984, henceforth HR; Raga & Böhm 1985, henceforth RB; Hartigan, Raymond, & Hartmann 1987, henceforth HRH; Noriega-Crespo, Böhm, & Raga 1989). Their proper motions exceed 300 km s^{-1} (Herbig & Jones 1981), and line widths of some knots reach 250 km s^{-1} (HR). The correlation of line widths with the excitation of many of the knots (as judged by the [O III]/Hβ ratio) fits nicely into the bow-shock picture, and the line profiles bear a respectable, although imperfect, resemblance to bow-shock model predictions (HR; RB; HRH). In these models, a bullet or jet drives a roughly paraboloidal shock wave into the ambient cloud. At the bow-shock surface, gas encounters an oblique shock. The normal component of its velocity is the effective shock speed (determining the postshock temperature), and the parallel component is conserved (contributing to the shape of the line profile). These models are especially successful with relatively simple bow-shock structures such as HH 30 (Morse et al. 1992).

However, HH 2 has turned out to be far more complex than envisioned in the early bow-shock models. The *Hubble Space Telescope* (*HST*) images of Schwartz et al. (1993) show high-contrast structure down the resolution limit—tiny, dense knots presumably created by Kelvin-Helmholtz or thermal instabilities (e.g., Blondin, Königl, & Fryxell 1989; Stone & Norman 1993; de Gouveia Dal Pino & Benz 1993). Very dense, cold ambient material seen in ammonia emission might also fragment the flow (Torrelles et al. 1992). The UV spectrum of HH 2 shows the anticipated C IV emission (Böhm et al. 1987; Raymond, Hartigan, & Hartmann 1988, henceforth RHH), but not the N V. The blue continuum observed in the optical matches the prediction of H 2γ emission from neutrals excited as they enter the shock (Dopita, Binnette, & Schwartz 1982), but the continued rise shortward of 1450 Å cannot be accounted for by 2γ emission. Infrared H_2 lines show intensity ratios corresponding to 2500 K, as might be expected in a C shock or a J shock with an MHD precursor (Elias 1980), but the association of H_2 emission with very high excitation knots is surprising (Davis, Eislöffel, & Ray 1994; Curiel 1992).

Here we present an ultraviolet spectrum of HH 2 obtained with the Hopkins Ultraviolet Telescope (HUT) during the Astro-2 mission. It covers the 912–1800 Å range with better resolution and signal to noise than the *IUE* spectra. It confirms the C IV and O III] emission reported by Böhm et al. and RHH, but we do not detect the O VI emission expected from a 200 kms^{-1} bow shock. The HUT spectrum shows that the continuum seen by *IUE* below 1650 Å is largely a blend of H_2 emission bands. At wavelengths below 1200 Å, the Lyman band features at 1053 Å and 1101 Å stand out clearly. Many levels of H_2 are excited, unlike the situation in Burnham's Nebula, HH 43 and HH 47 (Brown et al. 1981; Schwartz 1983; Curiel et al. 1996), where *IUE* and Goddard High-Resolution Spectrograph (GHRS) spectra show selective excitation by Lyα. The difference may result from higher densities and larger velocity dispersion in HH 2 than in the other objects. We discuss interpretations based on collisional excitation of molecules passing through the shock and on Lyα fluorescence when the line width is large and many ro-vibrational levels are available to absorb photons. Neither is entirely satisfactory.

2. OBSERVATIONS AND DATA REDUCTION

HUT was flown as part of the Astro-2 space shuttle mission in 1995 March. It obtained 2–4 Å resolution spectra of many types of astronomical objects over the wavelength range 850–1840 Å. Its 0.9 m primary mirror feeds a prime-focus spectrograph with a photon-counting detector. The instrument is described in Davidsen et al. (1992) as it was flown on Astro-1. For the Astro-2 mission, the primary mirror and the grating were coated with higher efficiency SiC coatings, which improved the throughput considerably (Kruk et al. 1995). The radiometric calibration was derived from laboratory measurements and from observations of hot white dwarfs during flight, and it is believed to be accurate to 5% over the entire wavelength range.

HH 2 was observed on 1995 March 13. The observation straddled the day-night terminator. To minimize contamination by airglow lines prominent in the sunlit portion of the orbit, we used the 12″ diameter aperture during the day, and then, to maximize the source counting rate, switched to the 20″ aperture during the night. The observations were centered on HH 2H ($05^h39^m59^s.7$, $-6°49'02''$ 1950), with pointing accuracy and stability of about $\pm 1''$. Totals of 1116 and 1098 s of good data were obtained during the day and night, respectively. The 12″ diameter aperture is sufficiently large for some photons to have been detected from HH 2D, but HH 2A′ should have been excluded. With the 20″ aperture, most of HH 2 was sampled, with the exception of the low-excitation knots HH 2E, HH 2K, and HH 2L. Böhm et al. (1987) found that the C IV emission-line region of HH 2H was unresolved at the 5″ resolution of *IUE*, while the continuum emission was somewhat more extended.

Figure 1 displays the 20″ and 12″ spectra. They appear to be identical, except that the 12″ spectrum shows about half as much flux, much stronger airglow features, and narrower spectral features, corresponding to the smaller aperture. Therefore, we will base the following discussion on the 20″ spectrum. Figure 2 shows this spectrum on an expanded scale, along with identifications for the stronger features. Table 1 lists the fluxes of several emission lines and continuum bands. The fluxes of complex features were measured with the SPECFIT task in the HUT package in IRAF (Kriss 1994). SPECFIT allows us to specify wavelength differences and intensity ratios when fitting Gaussian profiles to doublets or blended features (the N V doublet, O VI, and Lyβ). The reddening correction is a major uncertainty. Estimates based on different [S II] line ratios range from $E(B-V) = 0.11$ (HR) to $E(B-V) = 0.37$ (Brugel, Böhm, & Mannery 1981). Rather than the average Galactic extinction curve, the extinction curve derived by Bohlin & Savage (1981) for θ Ori is generally assumed for HH 1 and HH 2 (Brugel et al. 1981). Table 1 includes fluxes corrected for $E(B-V) = 0.11$ and $E(B-V) = 0.37$ with the θ Ori curve. For wavelengths below 1200 Å, we assume the wavelength dependence of Cardelli, Clayton, & Mathis (1989), normalized to the θ Ori curve at 1250 Å. The extinction correction has only a modest effect on the relative intensities of the UV features, but the uncertainty in comparing UV fluxes to optical or IR intensities is a factor of 2.5.

The HUT spectrum can be compared with *IUE* spectra of HH 2H (Böhm et al. 1987) and HH 2A′ (RHH). The C IV fluxes of the HUT spectrum and RHH agree to 10%, but fainter lines disagree badly. This is probably because of different aperture shapes, uncertainty in blind offset positions, and uncertain continuum placement in measuring line fluxes. HUT also detects the N III] multiplet that was lost in the noise of the *IUE* spectra, along with the O III] doublet that was seen in the HH 2H spectrum but was not

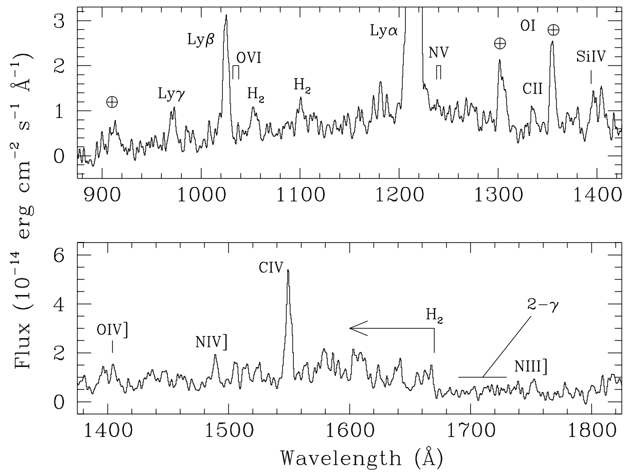

FIG. 2.—Spectrum obtained through the 20″ aperture with prominent features identified.

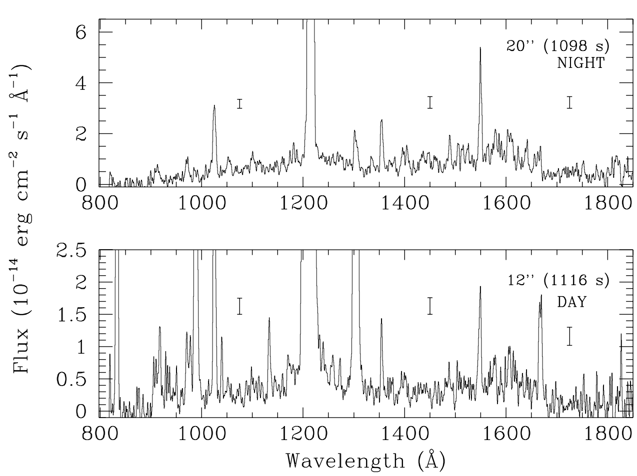

FIG. 1.—HUT spectra of HH 2 obtained through the 20″ diameter aperture (during orbital night) and the 12″ aperture (during orbital day). The spectra are plotted in 0.51 Å bins after smoothing with a Gaussian function of 1.5 pixel Gaussian width. Typical error bars based on the counting statistics per 0.51 Å bin are shown offset from the data at 1075, 1450, and 1725 Å.

TABLE 1

HH 2 FLUXES (10^{-14} ergs cm)$^{-2}$ s^{-1}

Wavelength (Å)	Ion	F_λ	$I_{0.11}$[a]	$I_{0.37}$[a]
977	C III	≤1.4	≤3.6	≤31.1
1034	O VI	≤1.3	≤3.1	≤22.5
1053.8	H_2	5.1	11.8	84.7
1101.5	H_2	5.0	9.1	64.5
1240	N V	≤0.3	≤0.6	≤2.4
1336.3	C II, H_2	2.6	4.5	16.1
1397/1405	Si IV, O IV], H_2	11.7	19.3	62.0
1489.1	N IV]	5.2	8.6	27.6
1549.5	C IV	20.6	34.0	111.0
1607.0	H_2	12.6	20.7	66.8
1640.5	H_2, He II	6.0	9.8	31.8
1663/1668	O III]	6.1	10.7	32.5
1752.0	N III]	3.5	5.7	18.6
1671–1742	H 2γ	30.6	50.2	162.0
1040–1186	H_2	106.0	229.0	1760.
1250–640[b]	H_2	175.0	290.0	936.0

[a] Corrected for reddening $E(B-V) = 0.11$ or 0.37, as described in text.

[b] Two-photon continuum and emission lines have been subtracted.

clearly visible in HH 2A′. No emission was detected in the C III λ977, O VI λλ 1032, 1038, or N V λλ1238, 1242 lines, however.

The HUT spectrum shows geocoronal Lyman lines and lines of O I. There is a broad hump centered near 1500 Å and a fainter, fairly flat continuum longward of 1680 Å. The spectrum confirms the argument of Böhm et al. (1987) that the faint continuum seen by *IUE* is real, along with their interpretation of it as H_2 emission. The features at 1053 and 1101 Å in the HUT spectrum are clearly the H_2 blends expected at these wavelengths. However, Böhm et al. took the 1500 Å hump to be continuum radiation produced during dissociation, while the HUT spectrum shows a blend of many H_2 lines. The broad hump near 1500 Å appears somewhat brighter in the HUT spectrum, but the shape is very similar to that seen with *IUE*. We do not detect any of the H_2 Lyman emission features pumped by Lyβ that are seen in the spectrum of Jupiter (Feldman et al. 1993). The reason is probably the efficient conversion of Lyβ to Hα plus a 2γ pair when Lyβ photons are absorbed by H atoms. The 2γ continuum, mostly caused by direct excitation of neutrals passing though the shock (Dopita et al. 1982), accounts for the continuum at longer wavelengths, as the H_2 emission does not extend beyond about 1640 Å. The 1671–1740 Å band represents 4.8% of the 2γ flux, implying a total 2γ emission, about 65% larger than the value derived from *IUE* by RHH.

3. ANALYSIS

3.1. *Lack of* O VI *Emission*

As described above, we did not detect the O VI doublet at 1032 and 1038 Å, and the upper limit is about 20% of the C IV flux. According to theoretical models of bow shocks, the full width at zero intensity of the emission lines should equal the bow-shock velocity, and for HH 2A′ and HH 2H, that implies $v_{\rm bs} \simeq 190$–250 km s^{-1} (HRH). The bow-shock models then predict I(O VI)/I(C IV) to be at least 2. Even with allowance for uncertain reddening, the lack of O VI emission contradicts the models. It is conceivable that molecular hydrogen attenuates the O VI lines. Jenkins & Peimbert (1997) list H_2 lines at λλ 1037.149, 1031.192. These are unlikely to affect seriously the O VI lines 0.5 and 0.7 Å away. However, the IR emission lines of H_2 imply substantial populations in vibrationally excited levels that are not usually observed in absorption. While this possibility should be investigated further, we have no basis yet for assuming that H_2 could so completely obliterate the very broad O VI doublet lines.

The complex small-scale structure discovered in *HST* images of HH 2 (Schwartz et al. 1993) at first glance offers a reason for discounting the bow-shock models, as there is no evidence at all for a classic bow-shock shape (although the pointlike feature seen in [O III] could simply be an unresolved bow shock). A more fundamental point, however, is that the complex structure does not change the overall energetics or the fact that reasonable oblique-shock geometries still imply that the line width equals the maximum shock velocity. This is a purely geometrical argument, in that the maximum line-of-sight velocity generated by an oblique shock moving in the plane of the sky (as is the case for HH 1 and HH 2) is max $(v_{\rm bs} \sin\theta \cos\theta) = v_{\rm bs}/2$. The most likely explanation for the discrepancy is a serious departure from the plane-parallel, steady-flow shock models used to construct the bow-shock models. Possibilities include a large neutral (or even molecular) fraction at the shock front (RHH), a flow time smaller than the radiative cooling time, or turbulent mixing of hot and cool gas by shear-generated turbulence (e.g., Slavin, Shull, & Begelman 1993).

The effects of neutrals entering a shock wave were computed by Cox & Raymond (1985). In fully neutral gas, a 200 km s^{-1} shock produces a spectrum like that of a 185 km s^{-1} shock with additional H I emission. Since only shocks faster than 170 km s^{-1} produce O VI, this reduction in effective shock velocity significantly reduces the O VI emission. However, it is difficult to see how the preshock gas can remain neutral in the presence of the ionizing radiation from a shock that emits C IV. Models of the ionization state ahead of a 200 km s^{-1} bow shock show a negligible neutral fraction near the tip of the bow shock and modest changes in the UV line ratios (RHH).

Departures from plane-parallel, steady-flow shock models could arise from thermal instabilities or from a flow time smaller than the radiative cooling time. The former has only a modest effect on UV line ratios (Innes 1992). The latter could make adiabatic cooling significant, lowering the emission from the highest ionization states. The small size of the knots seen with *HST* (Schwartz et al. 1993) does imply a small flow time, but it also requires high densities and therefore a short radiative cooling time. The structure is so complex that it is difficult to estimate either the flow time or the radiative cooling time with confidence.

Turbulent mixing of the shocked interstellar medium (ISM) and shocked jet (or bullet) material is nearly unavoidable, but its consequences for the spectrum are hard to predict. It is not clear that the hot and cool components of the gas will mix with each other, and it is not at all obvious that mixing will reach scales small enough to average the electron temperatures in a time shorter than the radiative cooling time. A signature of strong mixing might be high-excitation emission lines from low stages of ionization. Unfortunately, the O I] λ1355 line is lost under geocoronal emission. Without detailed models for HH 2 parameters, it is difficult to assess the importance of mixing.

3.2. *Molecular Hydrogen Emission*

The detection of H_2 bands below 1200 Å, as well as the noisy but significant band structure seen at longer wavelengths (e.g., 1610, 1510, and 1580 Å), shows that the UV continuum detected by *IUE* below 1600 Å is in fact H_2 emission. At longer wavelengths, the continuum is consistent with hydrogen 2γ emission that is produced largely by collisional excitation to the 2*s* level, as expected for shocks encountering largely neutral gas (Dopita et al. 1982; Cox & Raymond 1985). The identification of H_2 emission resolves the question of the "blue continuum" investigated by Böhm et al. (1987). The latter was identified as an H_2 dissociation continuum by Böhm et al. (1987), because it lacks the dominant Lyman emission features reported by Schwartz (1983) in HH 43 and HH 47. Those objects showed strong emission in a set of transitions pumped by Lyα (1258, 1272, 1431, 1446, 1505, 1547, and 1562 Å), as has been seen in spectra of Burnham's Nebula (Brown et al. 1981) and predicted by Shull (1978). Several of these features can be seen in Figure 1, but they were not apparent in the *IUE* spectra. Curiel et al. (1996) observed a small part of the UV spectrum of HH 47 at higher resolution with GHRS. They confirmed the expected Lyα fluorescence transitions at

1270.98, 1271.83, and 1293.75 Å, but found an unexpected feature at 1293.35 Å as well.

The HUT spectrum of HH 2 clearly shows that molecular hydrogen produces most of the UV emission below 1620 Å. The dissociation continuum undoubtably contributes, but a substantial fraction of the molecular emission originates in bound-bound transitions. The mystery is why the spectrum looks so different from the HH 43 and HH 47 spectra. One possibility is that Lyα fluorescence produces the H_2 emission in HH 2 as well as in the other objects, but that the Lyα photons pump a much larger set of levels in HH 2. Another possibility is that the H_2 emission is produced by collisional excitation. We consider these excitation mechanisms in turn.

3.2.1. *Lyα Fluorescence*

The fluorescence spectrum seen in HH 43 is created by a single pumping transition, B–X (1–2) $P(5)$, at $+99$ km s^{-1} from Lyα line center (Schwartz 1983). Black & van Dishoeck (1987) list about 40 other possible pumping transitions. It seems plausible that the 100 km s^{-1} width in HH 47 (Hartigan, Raymond, & Meaburn 1990) makes it possible to pump one or two more transitions than possible in HH 43, each giving rise to a set of emission lines. HH 2, with a 200 km s^{-1} line width, could distribute the converted Lyα photons among a still larger number of lines. This interpretation can be checked against the energetics. Based on shock-wave models (HRH), we can infer the Lyα luminosity from the Hα luminosity. Taking a distance of 500 pc (which actually scales out of the comparison with molecular luminosity), $L_{\mathrm{H}\alpha} = 2.6\text{–}5 \times 10^{31}$ ergs s^{-1} for HH 2A′, HH 2H, and the fainter knots within the 20″ aperture. Scaling the 200 km s^{-1} bow-shock model of HRH to the Hα luminosity (the ratio is fairly insensitive to the choice of model), $L_{\mathrm{Ly}\alpha} = 5\text{–}10 \times 10^{32}$ ergs s^{-1}. This is consistent with the 2γ/Lyα ratios of the HRH models and the 2γ flux in Table 1, at least for the lower reddening value. The luminosity of the H_2 emission is $2\text{–}10 \times 10^{32}$ ergs s^{-1}, depending on the reddening correction, therefore at least 20% of the Lyα photons must be fluoresced in order to match the observed brightness. Thus Lyα fluorescence is energetically possible with the lower reddening value, but 100% efficiency is required for the larger reddening estimate.

The second test of the viability of fluorescent pumping of a large number of transitions is the optical depth of the transitions to be pumped. Since a large fraction of the Lyα luminosity must be converted, the optical depths of the pumping transitions must be of order unity. We can determine the optical depths by consideration of the infrared emission. Elias (1980) reports a flux of 1.5×10^{-13} ergs cm^{-2} s^{-1} from a 10″ diameter aperture centered on HH 2H in the (1–0) $S(1)$ line. Based on the images of Davis et al. (1994), we assume that this flux arises from about $\frac{1}{3}$ of the 10″ region. We can estimate the column density of the upper state from the flux and the A value of the transition (Turner, Kirby-Docken, & Dalgarno 1977) to obtain $N(v, J = 1, 1) = 10^{16}$ cm^{-2}. The lower level of the B–X (1–2) $P(5)$ transition lies 0.6 eV higher, so even with a Boltzmann distribution of populations at a typical temperature $T = 2500$ K (e.g., Brand 1995), its column density is less than 10^{15} cm^{-2}. For an absorption oscillator strength of 0.029 (Black & van Dishoeck 1987) and a line width of 30 km s^{-1}, this gives an optical depth of 3.0. A smaller line width would imply a larger optical depth, but the line would intercept a correspondingly smaller fraction of the Lyα photons.

Most of the potential pumping transitions arise from higher lying vibrational levels. Each vibrational level is about 0.5 eV above the last, so that the populations drop by an order of magnitude for each vibrational level. Thus transitions arising from vibrational levels 4 and above should be optically thin, leaving only three potential pumping transitions in the Black & van Dishoeck list. We conclude that fluorescence probably cannot produce a broad enough distribution of lines to match the observations.

3.2.2. *Collisional Excitation*

Böhm et al. (1987) also remarked that collisional excitation of H_2 by electrons might account for the UV emission of HH 2H. Liu & Dalgarno (1996) have computed theoretical H_2 emission spectra for a variety of H_2 temperatures and electron energies. The prediction for 1000 K H_2 and 20 eV electrons resembles the H_2 spectrum of HH 2 quite closely. Figure 3 shows the HUT spectrum with the Liu & Dalgarno model scaled to match the emission below 1200 Å and the spectral shape of hydrogen 2γ emission matched to the long-wavelength continuum. Both the observations and the model show discrete features at 1053 and 1101 Å and a blend of weak features at longer wavelengths out to the observed cutoff near 1640 Å, with a broad minimum between 1300 and 1450 Å. Most of the Liu & Dalgarno spectra have a dominant strong emission feature near 1610 Å, but the combination of low electron energy and relatively high excitation of the molecules provides for excitation of a large number of states and divides the emission among a very large number of lines.

While the agreement is impressive, there are reasons for caution in this interpretation as well. From the observational point of view, reddening will reduce the short-wavelength emission, compared with the longer wavelength range, and H_2 absorption that is both local to HH 2 and along the line of sight will cut into some of the emission features, especially those at 1053 and 1101 Å. On the theoretical side, it is difficult to mix hydrogen molecules with hot electrons before dissociating the molecules. A shock wave might do it in principle, but there is now evidence that T_e is

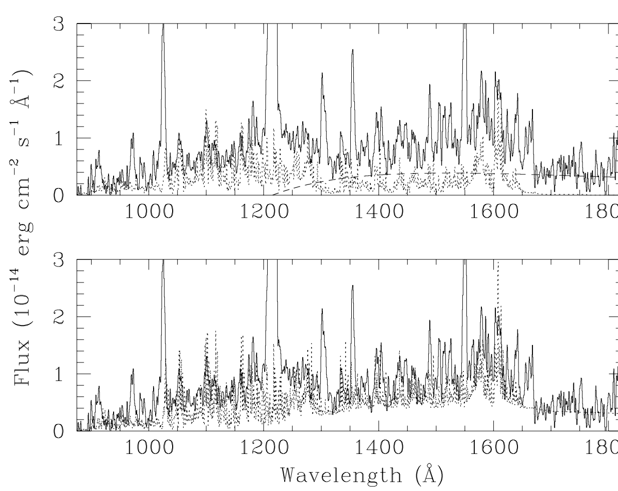

FIG. 3.—HUT spectrum with the 2γ spectral shape (*dashed line*) scaled to the long-wavelength continuum and the Liu & Dalgarno (1996) collisional excitation model (*dotted line*) scaled to the short-wavelength features.

low at the shock, and the electrons are gradually heated by Coulomb collisions with the ions (Laming et al. 1996). In the meantime, hot ions dissociate H_2 very rapidly.

The second problem is the molecular luminosity. Based on the estimate above, the observed portion of HH 2 produces over 10^{43} H_2 photons s^{-1}. For a preshock density of 500 molecules cm^{-3}, a shock velocity of 200 km s^{-1}, and a shock area of 10^{33} cm^2, this requires 1–5 photons $molecule^{-1}$. While excitation of the Lyman bands can produce 10 photons $molecule^{-1}$ (thanks to the small branching ratio to the vibrational continuum), excitations to the triplet states destroy molecules quite effectively. Even without collisions with protons or neutral atoms, it is unlikely that a molecule could produce more than three UV photons before being destroyed. Thus, it is necessary to mix hot electrons into molecular gas that is hot enough to excite the vibrational levels ($\simeq 1000$ K) but not hot enough to dissociate the molecules rapidly ($\simeq 10{,}000$ K). Neither a standard J shock nor a standard C shock (see Draine & McKee 1993) is well suited to this task. A J shock with an MHD precursor (Hartigan, Curiel, & Raymond 1989) might have the right properties, but sufficiently detailed models are not available, and it is difficult to see how an MHD precursor could exist at such high speeds and ionizing photon fluxes. Turbulent mixing is not an obviously better candidate.

Another implication of collisional excitation of the H_2 UV emission is the reduction of the energy available to heat the gas to O VI–producing temperatures. If the bow-shock tip encounters largely molecular gas, the effective shock velocity will drop enough to reduce the expected N V and O VI emission drastically. Again, it is difficult to see how molecules can survive the ionizing radiation field near the bow-shock tip, but such an effect would help resolve the issue of the missing N V and O VI emission in the HUT spectrum of HH 2.

4. CONCLUSIONS

The HUT spectrum of HH 2 shows several of the expected UV emission lines, but the N V and O VI emission predicted by 200 km s^{-1} bow-shock models is absent. This is a conflict not just with the details of the bow-shock models but also with the more general idea that a 200 km s^{-1} wide line profile requires 200 km s^{-1} radiative shock waves.

The HUT spectrum also shows discrete Lyman band emission below 1200 Å. It shows some band structure at longer wavelengths as well, pinning down the nature of the continuum seen with *IUE*. Both Lyα fluorescence and collisional excitation of H_2 may have attractive features for explaining the UV emission, but both have drawbacks as well. It is very hard to see how any MHD shock (a C shock or a J shock with a precursor) can exist so close to the ionizing flux of HH 2H. It is equally difficult to see how a J shock or turbulent mixing can produce H_2 UV photons efficiently enough to account for the observations.

This work was performed under NASA grant NAG8-1074 to the Smithsonian Astrophysical Observatory and NASA contract NAS5-27000 to Johns Hopkins University. The authors gratefully acknowledge the efforts of our colleagues on the HUT team, as well as the Astro-2 crew and the host of NASA personnel who worked on the mission. W. Liu provided the theoretical H_2 spectrum shown in Figure 3, and S. Curiel advised us on H_2 dissociation rates.

REFERENCES

Black, J. H., & van Dishoeck, E. 1987, ApJ, 322, 412
Blondin, J. M., Königl, A., & Fryxell, B. A. 1989, ApJ, 337, L37
Böhm, K.-H., Bürke, T., Raga, A. C., Brugel, E. W., Witt, A. N., & Mundt, R. 1987, ApJ, 316, 349
Bohlin, R. C., & Savage, B. D. 1981, ApJ, 249, 109
Brand, P. W. J. L. 1995, in Shocks in Astrophysics, ed. T. J. Millar & A. C. Raga (Dordrecht: Kluwer), 27
Brown, A., Jordan, C., Millar, T. J., Gondhalekar, P., & Wilson, R. 1981, Nature, 290, 34
Brugel, E. W., Böhm, K.-H., & Mannery, E. 1981, ApJS, 47, 117
Cardelli, J. A., Clayton, G. C., & Mathis, J. S. 1989, ApJ, 345, 245
Cox, D. P., & Raymond, J. C. 1985, ApJ, 298, 651
Curiel, S. 1992, in IAU Symp. 150, Astrochemistry of Cosmic Phenomena, ed. P. D. Singh (Dordrecht: Kluwer), 373
Curiel, S., Raymond, J. C., Wolfire, M., Hartigan, P., Morse, J., Schwartz, R. D., & Nisenson, P. 1995, ApJ, 453, 322
Davidsen, A. F., et al. 1992, ApJ, 392, 264
Davis, D. J., Eislöffel, J., & Ray, T. 1994, ApJ, 426, L93
de Gouveia Dal Pino, E. M., & Benz, W. 1993, ApJ, 410, 686
Dopita, M. A., Binnette, L., & Schwartz, R. D. 1982, ApJ, 261, 183
Draine, B. T., & McKee, C. F. 1993, ARA&A, 31, 373
Elias, J. H. 1980, ApJ, 241, 728
Feldman, P. D., McGrath, M. A., Moos, H. W., Durrance, S. T., Strobel, D. F., & Davidsen, A. F. 1993, ApJ, 406, 279
Hartigan, P., Curiel, S., & Raymond, J. C. 1989, ApJ, 347, L31
Hartigan, P., Raymond, J. C., & Hartmann, L. 1987, ApJ, 316, 323
Hartigan, P., Raymond, J. C., & Meaburn, J. 1990, ApJ, 362, 624
Hartmann, L. W., & Raymond, J. C. 1984, ApJ, 276, 580
Herbig, G. H., & Jones, B. F. 1981, AJ, 86, 1232
Innes, D. E. 1992, A&A, 256, 660
Jenkins, E. B., & Peimbert, A. 1997, ApJ, 477, 265
Kriss, G. A. 1994, in ASP Conf. Ser. 61, Astronomical Data Analysis Software and Systems III, ed. D. R. Crabtree, R. J. Hanisch, & J. Barnes (San Francisco: ASP), 437
Kruk, J. W., Durrance, S. T., Kriss, G. A., Blair, W. P., Espey, B. R., & Finley, D. S. 1995, ApJ, 454, L1
Laming, J. M., Raymond, J. C., Blair, W. P., & McLaughlin, B. M. 1996, ApJ, 472, 267
Liu, W., & Dalgarno, A. 1996, ApJ, 467, 446
Morse, J. A., Hartigan, P., Cecil, G., Raymond, J. C., & Heathcote, S. 1992, ApJ, 399, 231
Noriega-Crespo, A., Böhm, K.-H., & Raga, A. C. 1989, AJ, 99, 1918
Raga, A. C., & Böhm, K.-H. 1985, ApJS, 58, 201
Raymond, J. C., Hartigan, P., & Hartmann, L. 1988, ApJ, 326, 323
Schwartz, R. D. 1977, ApJ, 212, L25
———. 1983, ApJ, 268, L37
Schwartz, R. D., et al. 1993, AJ, 106, 740
Shull, J. M. 1978, ApJ, 224, 841
Slavin, J. D., Shull, J. M., & Begelman, M. C. 1993, ApJ, 407, 83
Stone, J. M., & Norman, M. L. 1993, ApJ, 413, 210
Torrelles, J. M., Rodríguez, L. F., Cantó, J., Anglada, G., Gómez, J. F., Curiel, S., & Ho, P. T. P. 1992, ApJ, 396, L95
Turner, J., Kirby-Docken, K., & Dalgarno, A. 1977, ApJS, 35, 281